acta physica slovaca vol. 44 No. 6, 465 – 476 December 1994

THE FAST PARTICLES SPECTRUM IN FLUID DYNAMICS MODEL OF HEAVY ION COLLISIONS

A. T. D'yachenko
V. G. Khlopin Radium Institute, Shvernik 28, 194021 St. Petersburg, Russia[1]

Received 4 August 1993, in final form 12 August 1994, accepted 22 September 1994

The fluid dynamics model of heavy ion collisions in the 10-100 MeV/nucleon energy range is used to calculate double differential inclusive cross sections for nucleon production. The calculated nucleon spectra are shown to describe experimental data in the energy range considered for all observable angles. The model assumes the existence of the source of high energy particles with the velocity equal to one half of the beam particle velocity.

1. Introduction

We consider here the fluid dynamics model of heavy ions collisions in the energy range 10–100 MeV/nucleon. This process is under active investigation [1-5], being connected with a hope to produce a nuclear system at high temperature and to observe reaction dynamics which is significantly different from that at much lower or much higher energies. In this transition energy regime, one should expect the evolution of the reaction mechanism from dynamics dominated by mean–field phenomena to that determined by nucleon–nucleon collisions.

At present the methods of computation of various processes of nucleus–nucleus interaction have reached a considerably high level [6,7]. However, for better understanding of the physical picture of nucleus-nucleus interactions in this energy region, some additional research is necessary. One of the specific features of the process is the fast particles source with the velocity equal to one half of projectile velocity.

The conventional evaluations of the applicability of the fluid dynamics approach are based on the comparison of the mean free path length λ of a nucleon in composite system with the characteristic dimensions of the formed systems L. The validity condition can be expressed as [8,9]

$$\frac{\lambda}{L} \sim \frac{1}{\sigma_{NN}\rho R} \sim \frac{\rho_0}{\rho} A^{-1/3} << 1, \qquad (1)$$

[1]E-mail address: ARK@RI.SPB.SU

where σ_{NN} is the nucleon-nucleon interaction cross section, ρ, ρ_0 are the equilibrium and nonequilibrium nucleon densities respectively, R is the nuclear radius, and A is the mass number.

The condition (1) is obtained neglecting the Pauli principle. At low energies ($E_0 \sim$ 10-20 MeV/nucleon), the Fermi liquid effects are important [10]. They are described by the equations of the time dependent Hartree–Fock method [11], or by the Vlasov equation in the quasiclassical limit (see, e.g. [12]) or by simplified equations in the framework of the long mean free path fluid dynamics [13].

The equations of long mean–free–path fluid dynamics obtained in [14] lead to results which are close to those of the time dependent Hartree–Fock method [11].

Further natural development of this approach was the combination of two models: the "non-collisional" fluid dynamics [15] and the conventional local equilibrium fluid dynamics [16], derived in [17] in the τ-approximation according to Bertsch's parametrization [18].

In addition to the results obtained earlier [14,17] the side motion of nuclear media is taken into account in this paper. We consider here a wider energy range for both very asymetric combination of colliding nuclei and for a collision of two identical nuclei. Satisfactory agreements with experimental double differential cross sections $d^2\sigma/d\Omega dE$ of secondary nucleon emission at small as well as at large angles has been obtained.

It is known [2,19-24] that the light particles emission provides an important information on the complex nuclei interaction mechanism. The experimental data show essential increase of the high energy particles yield in comparison with the evaporation model calculations.

A number of different models was suggested to describe heavy ion reactions at these energies: the cascade, the thermodynamical, and the direct reactions models as well as some others (see, e.g. [20-25]). Our approach is close to that of the hot–spot model, proposed by H.A. Bethe as early as in 1938 [25].

Parameters of the model are not uniquely determined. Other similar thermodynamic models – fireball and firestreak models do not take into consideration the collective motion of nuclear matter. They require fitting parameters and lead to overestimation of temperature and yields of secondaries.

The time evolution of the hot spot is described here without any free parameters.

2. Fluid dynamic stage

The nonrelativistic fluid dynamic equations are used here to describe the interaction of heavy ions with energies $E < 300$ MeV/nucleon [14,17].

In the low energy region it is impossible to satisfy the condition (1) of local thermodynamic equilibrium because of the Pauli principle. Nevertheless in this case it is possible to obtain the equations of the long mean–free–path fluid dynamics.

The unification of the two models for the equation of state is carried out for the times comparable with the relaxation time $\tau_{\rm rel}$, obtained in [18].

The equations of fluid dynamic are known to be valid also for Fermi liquid, but the distribution function and the equation of state depend on how close the system is to the state of local equilibrium.

Considering nuclear system as Fermi liquid [10], Bertsch found [18] that

$$\tau_{\rm rel} = \sigma_{NN} v_F \rho \frac{3.3 E_i}{E_F}, \tag{2}$$

where $E_F = 37 MeV$, $v_F = \sqrt{\frac{2E_F}{m}}$, $\rho = 0.15 fm^{-3}$, $\sigma_{NN} = 40$ mb. The relaxation time is expressed through the exitation energy E_i (MeV/nucleon) and does not depend on the form of this energy (this energy is composed of the deformation energy of the Fermi sphere and the thermal energy). The $\tau_{\rm rel}$ can be approximately expressed through the initial collision energy per nucleon E_0 [18]

$$\tau_{\rm rel} = \frac{3}{E_0} 10^{-21} c. \tag{3}$$

Comparing $\tau_{\rm rel}$ and $\tau_c \sim L/c_s$, where τ_c is characteristic time of the collision process (L is the mean characteristic longitudinal size of the formed system, c_s is the sound velocity in nuclear matter), one can conclude that for energies 10-20 MeV/nucleon $\tau_{\rm rel} > \tau_c$. The most suitable equation of state is the equation of state with anisotropic pressure tensor in this case. With an increase of the collision energy the estimate becomes $\tau_{\rm rel} < \tau_c$, what justifies the validity of the local equilibrium fluid dynamics with the isotropic equation of state.

Equations obtained in ref.[17] take into account the transition from the initial nonequilibrium state to the local equilibrium with increasing of the collision energy. The equation of state determining the dependence of the pressure p and the energy density e on the density ρ is a sum of kinetic terms and interaction terms, $p = p_{\rm kin} + p_{\rm int}$ and $e = e_{\rm kin} + e_{\rm int}$. The contributions of the interaction terms (we chose the Skyrme–type interaction) to the pressure and the energy density are

$$p_{\rm int} = \frac{3}{8} b_0 \rho^2 + \frac{1}{8} b_3 \rho^3 \ , \ e_{\rm int} = \frac{3}{8} b_0 \rho^2 + \frac{1}{16} b_3 \rho^3, \tag{4}$$

where ρ is the nuclear density, b_0 and b_3 are effective interaction parameters ($b_0 = -1089$ MeV fm^3,$b_3 = 17270$ MeV fm^6). The form of the kinetic terms depends on of the relaxation rate of the excited nuclear system. The longitudinal component of the anisotropic pressure tensor can be written as follows:

$$p_{\rm kin} = \frac{\hbar^2}{5m} \left(\frac{3}{2} \pi^2 \rho_0 \right)^{\frac{2}{3}} \frac{\rho^3}{\rho_0^2} + 2I, \tag{5}$$

$$e_{\rm kin} = \frac{\hbar^2}{10m} (\frac{3}{2} \pi^2 \rho_0)^{\frac{2}{3}} ((\frac{\rho}{\rho_0})^2 + 2)\rho + I, \tag{6}$$

where $I = \int \delta f \frac{p^2}{2m} \frac{d^3p}{(2\pi\hbar)^3}$ is the effective thermal energy density .

For the isotropic pressure

$$p_{\rm kin} = \frac{\hbar^2}{5m} (\frac{3}{2} \pi^2)^{\frac{2}{3}} \rho^{\frac{5}{3}} + \frac{2}{3} I, \tag{7}$$

$$e_{\rm kin} = \frac{3\hbar^2}{10m}(\frac{3}{2}\pi^2)^{\frac{2}{3}}\rho^{\frac{5}{3}} + I. \qquad (8)$$

In ref. [17], we considered the combination of these cases. The qualitative description of the nuclear fluid dynamics stage has been made in ref. [14], were we confined ourselves to almost central collisions, i.e. to small impact parameters. Moreover the description of the compression and dilution stages was carried out in Carthesian geometry, which does not allow to take into account the sideways motion of nuclear matter.

The improvement of the calculation was achieved by including collisions with large impact parameters, when the nuclei do not overlap completly, which is essential for collision of nuclei of close dimensions. The time evolution of overlapping parts is considered in the spherical coordinate system.

The computation of fluid dynamic flows is performed most easily in the reference frame, where the colliding nuclei are moving towards each other with equal velocities. The velocity of this system is equal exactly to one half of the projectile velocity v_0 ($v = v_0/2$). At the moment of impact the shock waves start to propagate from the bound surface. In the chosen reference frame the velocity of the shock wave D, the density ρ and the heat energy density I in the compression area are obtained from the conditions of the continuity the mass flow, the momentum flow and the energy flow at the shock wave front [14]. Strictly speaking, this stage requires microscopical description, but as mentioned above, the results of this model are close to those obtained with the time dependent Hartree-Fock method.

During time $t = L(s)/D$ (where $L(s)$ is longitudinal projectile space size, depending on the impact parameter s), the initially compressed matter undergoes sideway motion which can be determined from the mass and energy conservation in spherical coordinate system. This gives density ρ and radius R of a ball, formed in the overlapped area of the colliding nuclei ($R = c_s t$, where $c_s(\rho)$ is the sound velocity, depending on the density ρ). Generally speaking, the size R of the heated area depends on the impact parameter s and projectile energy and can be compared with the size of the projectile in average.

Spherical region formed undergoes the isoenthropic expansion (we neglect the viscosity and the thermal conductivity as the Reinold's number $Re > 1$), where pressure on free boundaries is equal to zero.

The influence of the angular momentum of the projectile is negligible here, since the time of the nuclear rotation is $\sim 10^{-21}$s, which is an order of magnitude higher than the characteristic time for the fluid dynamics stage.

The solution of the fluid dynamics equations in spherical coordinates is more complicated than in rectangular coordinates (see, e.g., [26]). It is possible to find an automodel (converging and diverging dilution waves) which are the nontrivial solutions of the fluid dynamics equations. The approximate general solution is the superposition of the simple dilution waves, which are radiated from the symmetry center $r = 0$ and from the boundaries of the sphere $r = R$. The dependence of the velocity $v(r,t)$ and of the sound velocity c_s on r and t is

$$v(r,t) = \frac{1}{2}(\frac{r}{t_1+t_2} + \frac{r-R}{t_1}), \qquad (9)$$

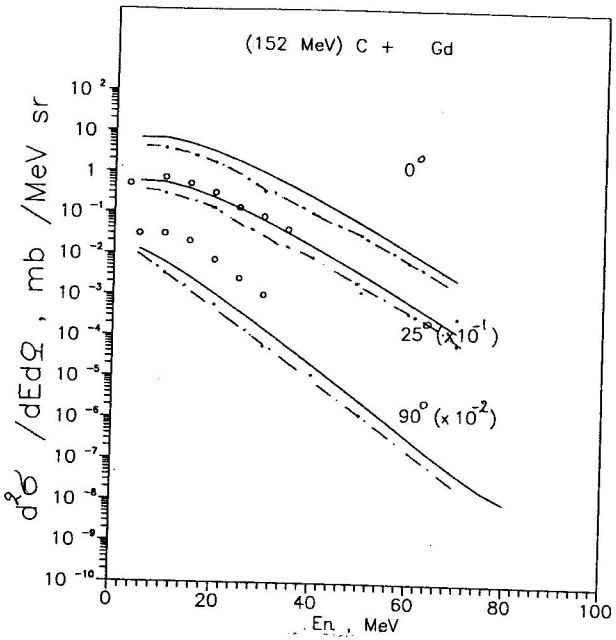

Fig.1: Spectra of neutrons calculated by averaging integral (11) (solid line), and the full calculation (11) (dash-dotted line), and the experimental (hard component - open circles) spectra of neutrons, emitted in the reaction $^{12}C + ^{158}Gd$ at E/A = 12 MeV at angles θ =0, 25, 90° [27].

$$c_s(\rho) = \frac{1}{2}(\frac{r}{t_1+t_2} - \frac{r-R}{t_1}), \qquad (10)$$

where t_1 is the time counted from the moment of the beginning of the dilution stage, $t_2 = R/c_s$ is the time for which the head dilution wave passes from the system boundary to the symmetry center.

Solutions (8)-(9) satisfy fluid dynamics equations with the accuracy not worse than 10 per cent, which is possible to check straightforwardly by substituting them into the initial equations.

The nontrivial solution is sewed with the trivial one $v = 0$ at $r = 0$, i.e. in the region of the constant flow.

The fluid dynamics has been completed, when the expanding nuclear system reaches the critical density $\rho^*(\rho^* = -2b_0/b_3)$, which is determined from the "instability" condition $dp_{\rm int}/d\rho = 0$ [14], at the moment of time t^*, which is different for each element of nuclear matter. At the moment t^* the breakup of the nuclear system into nucleons and fragments occurrs.

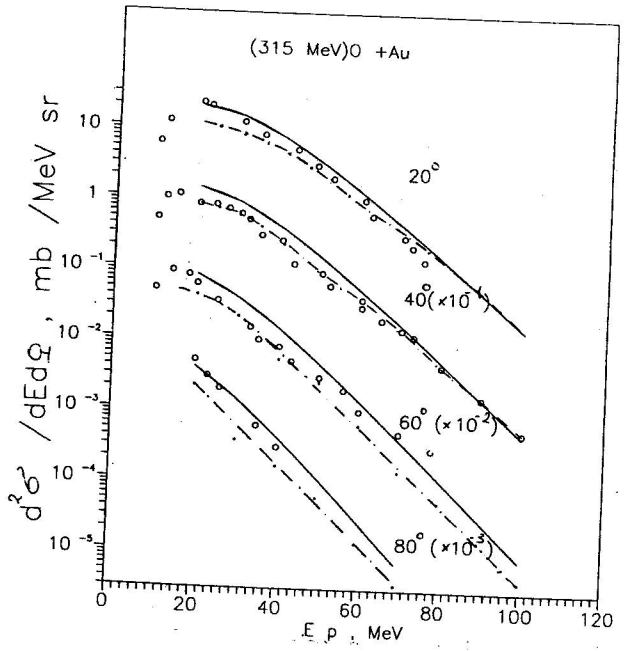

Fig.2: Spectra of protons calculated by the simplified method (solid line) and by the detailed calculation (dash–dotted line), the experimental spectra of protons (open circles), emitted in the reaction $^{16}O + {}^{197}Au$ at $E/A = 20$ MeV at angles $\theta = 20, 40, 60, 80°$ [28].

3. Particle emission spectrum

The double differential cross section of the secondary particles (nucleons) is equal to (s is the impact parameter)

$$d^2\sigma/d\Omega dE = \frac{2m\sqrt{2mE}}{(2\pi\hbar)^3}\int sds\int d\phi d\vec{r} f(E,\vec{r},t^*), \qquad (11)$$

where the distribution function $f(E,\vec{r},t^*)$ of the nucleons has the form

$$f(E,\vec{r},t^*) = (1+exp\left((\vec{p}-m\vec{v}_0/2-m\vec{v}(\vec{r},t^*))^2/2mT+(\chi-\mu)/T\right))^{-1}. \qquad (12)$$

Here, $\vec{v}(\vec{r},t^*)$ and $T(\vec{r},t^*)$ are the fields of the velocities and temperatures correspondently. These fields are the solutions of the fluid dynamics equations in the system of equal velocities of colliding nuclei, ϕ is the azimuthal angle in the laboratory system, $\mu(T)$ is the chemical potential, determined from the condition

$$\rho^* = \frac{4}{(2\pi\hbar)^3}\int(1+exp((\frac{p^2}{2m}-\mu)/T)^{-1}4\pi p^2 dp. \qquad (13)$$

Here $p=\sqrt{2mE}$ is momentum, $\mu(0)=E_F$ is the Fermi energy, χ is the energy shift, (difference of binding energy between the nuclear matter and that of a real nucleus)

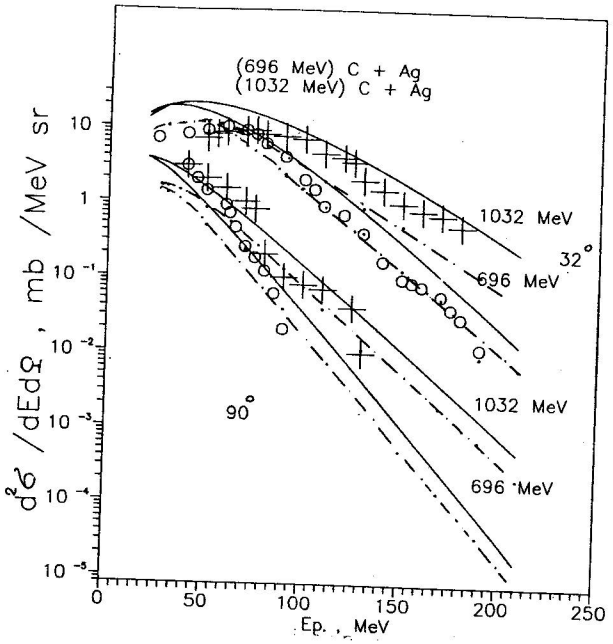

Fig.3: Spectra of protons calculated by the simplified method (solid line) and by the detailed calculation (dash–dotted line), the experimental spectra (open circles) at $E/A = 58$ MeV and (crosses line) at $E/A = 86$ MeV [29] for protons emitted in the reaction $^{12}C + {}^{108}Ag$ at angles $\theta = 32, 90°$.

The value χ denotes that the nucleon binding energy in a nucleus (~ 8 MeV) differs from that in nuclear matter ~ 15 MeV.

The expressions (11)-(12) describe neutrons. After the change $E \longrightarrow E - E_c$, where E_c is the Coulomb barrier for protons, these expressions become valid for protons.

We have performed calculations of double differential cross sections for various angles, according to expressions (11, 12) for reactions $A + B \longrightarrow p(n) + X$.

4. Comparison with experiment

Comparison of the calculated double–differential cross sections $d^2\sigma/d\Omega dE$ for nucleon emission with the experimental data for the reactions with ^{12}C and ^{16}O projectiles at energies 12, 20, 58 and 86 MeV/nucleon and with more massive nuclei La + La at 138 MeV/nucleon is presented in Fig.1-6.

In Fig. 1 the calculated neutron spectra (solid line) for the reaction $^{12}C+{}^{158}Gd$ at 152 MeV incident energy are compared with the treated hard component of experimental spectra [27] at angles 25 and 90° (open circles). The result of calculations according to expressions (11)-(12) are given by dash–dotted, the multiple integral being calculated by the Monte-Carlo method. Multiple integral is reduced to a usual one $\int d\phi d\vec{r}$ by averaging over internal angular variables (solid line).

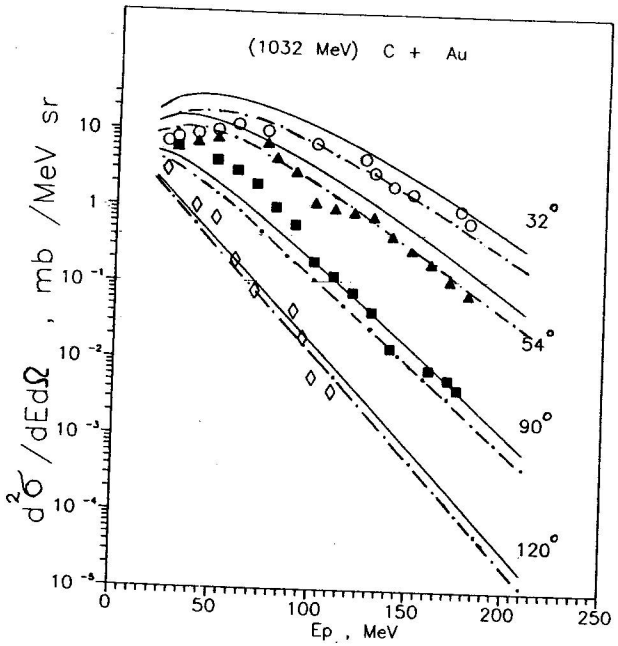

Fig.4: Spectra of protons calculated by the simplified method (solid line) and by detailed calculation (dash–dotted line), the experimental spectra [29] of protons emitted in the reaction $^{12}C + {}^{197}Au$ at $E/A = 86$ MeV at angles $\theta = 32, 54, 90, 120°$.

These two ways of calculation of the inclusive cross section (10) are in agreement with each other and also with the experimental data at $\theta = 25°$. The agreement with the experiment is worse at $\theta = 90°$.

The decrease of the cross section at the angle 90° may be caused by some simplification of the heavy–ion interaction mechanism at the relatively low collision energy (12 MeV/nucleon).

For the reaction $^{16}O + {}^{197}Au$ at 135 MeV incident energy, the calulated spectra are in satisfactory agreement with the experimental ones [28] at $\theta = 20, 40, 60, 80°$ (Fig. 2). Here the solid curve corresponds to the particle spectrum, calculated by averaging the momentum distribution over angular variables . The dash–dotted curve corresponds to the spectrum, calculated with the the full multiple integral (11). It should be noted, that τ_{rel} obtained at this energy is close to τ_c and the system is close to the state of local thermodynamic equilibrium.

The comparison of the calculation with the experimental data is shown also for the reactions, induced by ions ^{12}C at energies 58 and 86 MeV/nucleon [29].

Double differential cross sections for the emitted protons are shown for the reaction $^{12}C + {}^{197}Au$ at the energies 58 and 86 MeV/nucleon for $\theta = 32, 90°$ in Fig. 3. Spectra calculated by averaging over the angular variables are presented by solid curves. One can see that the calculated spectra coincide with the experimental ones but the calculations

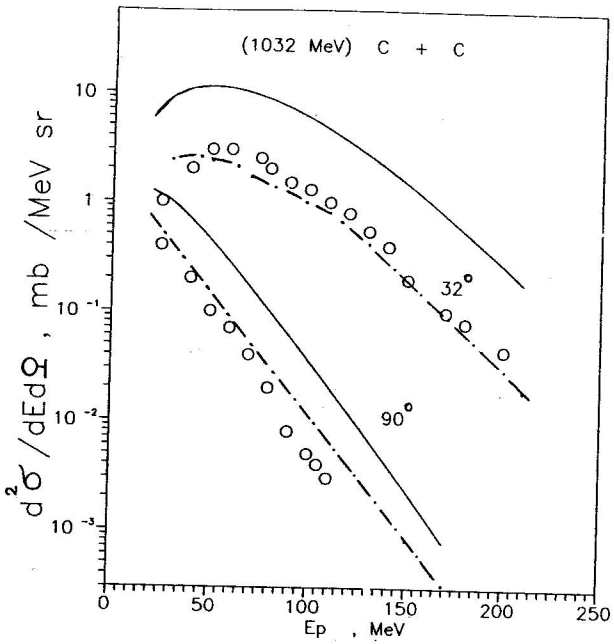

Fig.5: Proton spectra calculated by the simplified method (solid line) and by the detailed calculation (dash–dotted line), and experimental spectra (open circles) [29] of protons emitted in the reaction $^{12}C + {}^{12}C$ at $E/A = 86$ MeV at angles $\theta = 32, 90°$.

give somewhat over-estimated value for low proton energies at the angle $\theta = 32°$. The detailed calculation made on the basis of the integral (11) (dash–dotted line), gives the correct absolute value of the cross section at low proton energy.

The comparison of the calculated and the experimental spectra in the reaction $^{12}C + {}^{197}Au$ at energy 86 MeV/nucleon at the angles of emitted protons $\theta = 32, 54, 90, 120°$ (the notations for different variants of calculation are the same as in previous figure) is shown in Fig. 4. The correlation between the simplified calculation, the detailed calculation and the experimental data are the same as in previous figure. The detailed calculation gives the absolute value of cross section lower, than that of the simplified calculation, but it is still in satisfactory agreement with the absolute value of experimental cross section.

The comparison between the calculated and the experimental spectra is shown for the collision of identical nuclei $^{12}C + {}^{12}C$ at 86 MeV/nucleon (Fig. 5, experimental data from ref.[29]) and La + La at 138 MeV/nucleon (Fig. 6, experimental data from ref.[30]).

Fig. 5 repeats the main features of the interrelation between the calculated and the experimental cross sections at 32° and 90° (the notations are the same, as in previous figure). The simplified calculation gives the absolute value of the cross section more than the detailed calculation (dash–dotted line), which is in satisfactory agreement with

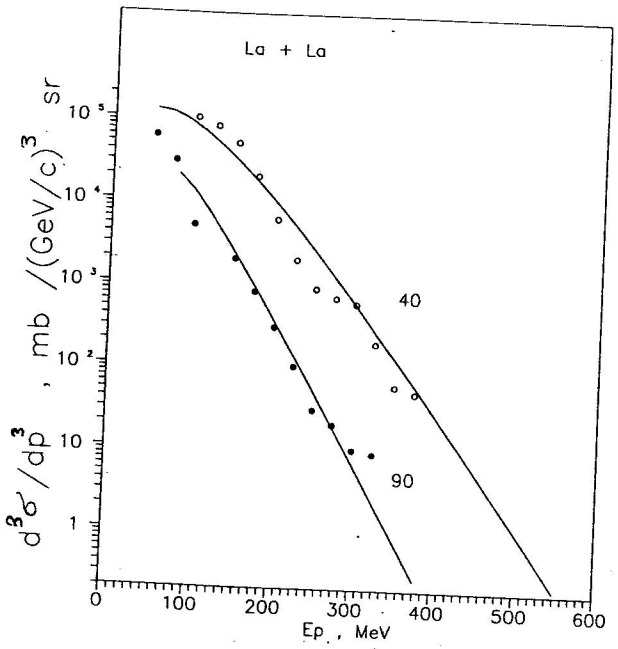

Fig.6: Proton spectra calculated by the simplified method (solid line), experimental spectra [30] of protons emitted in the reaction La + La at $E/A = 138$ MeV at angles $\theta = 40, 90°$.

the absolute value of the experimental cross section.

In Fig. 6 the calculated and experimental spectra [30] are compared for the reaction La + La at the energy 138 MeV/nucleon and angles $40, 90°$. For this case only relative values of the double–differential cross sections are studied, because the selection of the central events has been made in experiment. The experiment [30] is particulary important for checking the fluid dynamics model, because the collisions of the two sufficiently heavy nuclei are considered in [30], central events having been selected.

It is important to note, that we continue to simplify the calculation; after averaging we extract the exponential factor from the integral (11) and the cross section can be expressed as

$$d^2\sigma/d\Omega dE = \frac{2m\sqrt{2mE}}{(2\pi\hbar)^3}\pi {s_{max}}^2 \frac{4}{3}\pi R_m^3 exp(-\frac{(E - \sqrt{EE_o}\cos\theta + \alpha E_o - E_b)}{T}). \quad (14)$$

This corresponds to the existence of the source of secondary particles moving with the velocity, equal to one half of the beam particle velocity. Here, R ($R = c_s t$) is the average size of the heated region, coefficient $\alpha \sim 7/12$ ($\alpha = 1/3 + 1/4$) comes from the almost linear r–dependence of the velocity v (eq. (8)), E_b is the nucleon binding energy. The temperature of the source is related to the density of the thermal energy I at the dilution stage ($I = \frac{m}{2\hbar^2}(\frac{2}{3\pi})^{2/3}\rho^{*1/3}T^2$), as is usually done [14].

It is well-known [24] that experimental data concerning the spectra of light particles can be parametrized with the help of the set of sources with proper parameters. As follows from the previous considerations, the main contribution to the inclusive cross section comes from the "hot" source moving with the velocity nearly equal to one half of the beam particle velocity in agreement with the existing experimental data [28-29].

5. Conclusion

Thus, it is shown that the the fluid dynamics model is rather good for the description of the inclusive double differential cross sections for the emission of particles (nucleons) in the transition energy region 10–100 MeV/nucleon (to be more precise $>$ 20 MeV/nucleon). The results happen to be almost insensitive to the choice of the effective forces parametrization.

We note that the simplification of calculations resulting from averaging allows one to reveal the "hot" source of secondaries, moving with the velocity equal to one half of the projectile velocity in agreement with the existing experimental data.

It is clear that the model is not free from defects. It seems that the low neutron yield at the angle 90° at low energies $\sim$ 12 MeV/nucleon may be caused by the influence of the Coulomb field of the target on projectile, as well as by the contribution of some other peripheral mechanisms. The correlation of the relaxation time and the collision time at these energies leads to more complicated dynamics of Fermi liquid, than for higher energies.

It is important that all characteristics of the secondary particles spectra are calculated unambiguously in this model.

Acknowlegment The author is grateful to V.E.Bunakov and V.D.Toneev for their attention and critical remarks, to K.A.Gridnev, F.F. Karpeshin, O.V.Lozhkin, K.O. Oganesyan, Yu.E.Penionzhkevich for the interest to the work, and to A.A.Rimski-Korsakov, V.P.Eismont and S.G.Yavshits for useful discussions. The author would like to thank Professor Yu.Ts.Oganessian for support and hospitality while author's stay at Dubna in May 1993. He is also grateful to the Referee for his valuable comments.

References

1 G.N.Flerov: Int. School-Seminar on Heavy Ion Physics, Dubna, D7- 83- 644, (1983), 9.
2 D.K.Scott: Proc. Int. School on Nuclear Structure, Dubna, D4- 80- 385, (1980), 297.
3 G.D.Westfall et al.: Int. School-Seminar on Heavy Ion Physics, Dubna, E7-93-274, 2 (1993), 197.
4 G.F.Bertsch, S.Das Gupta: Phys. Rep. 160 (1988), 189.
5 D.H.E.Gross: Prog. Part. Nucl. Phys. 30 (1993), 155.
6 H.Stocker, W.Greiner: Phys. Rep. 137 (1986), 277.
7 I.N.Mishustin, V.N.Russkikh, L.M.Satarov: Yadernaya Fizika 54 (1991), 429.
8 V.G.Nosov, A.N.Kamchatnov: Zhurnal Experimentalnoi i Teoreticheskoi Fiziki 70 (1976), 768.

9 M.Yu.Ivanov, Yu.A.Kudeyarov, K.P.Stanyukovich, G.D.Shirkov: Yadernaya Fizika 25 (1977), 1292.
10 A.A.Abrikosov,I.M.Khalatnikov: Uspekhi Fizicheskikh Nauk 64 (1958), 177.
11 P.Bonche,S.Koonin,J.W.Negele: Phys.Rev. C13 (1976), 1226.
12 A.B.Larionov,I.N.Mishustin,V.N.Russkikh: Yadernaya Fizika 55 (1992), 2429.
13 V.M.Kolomietz,H.H.K.Tang: Phys. Scripta 24 (1981), 915; V.M.Kolomietz: Kollektivnaya yadernaya dinamika. Leningrad. Nauka (in Russian) 1990, 67.
14 A.T.D'yachenko,V.A.Rubchenya,V.P.Eismont: Izv. Akad. Nauk SSSR, ser. fiz. 45 (1981), 767; 2070.
15 G.Holzwarth: Phys. Lett. 66B (1977), 29.
16 C.Y.Wong,J.A.McDonald: Phys. Rev. C16 (1977), 1196.
17 A.T.D'yachenko: Izv. Akad. Nauk SSSR, ser. fiz. 51 (1987), 902.
18 G.Bertsch: Z. Phys. A289 (1978), 103.
19 Yu.Ts.Oganessian: Proc. Int. School on Nuclear Structure, Dubna,D4- 80- 385, (1980), 261.
20 R.V.Jolos: ibid, p. 277.
21 Yu.E.Penionzhkevich: Int. School-Seminar on Heavy Ion Physics, Dubna, D7- 83- 644, (1983), 279.
22 V.E.Bunakov,V.I.Zagrebaev: ibid, p. 288.
23 E.Betak,V.D.Toneev: Particles and Nuclei,Dubna, 12 (1981), 1432.
24 V.I.Zagrebaev,Yu.E.Penionzhkevich: Particles and Nuclei,Dubna,24 (1993), 295.
25 H.A.Bethe: Phys. Rev. 53 (1938), 267.
26 G.B.Whitham: Linear and Nonlinear Waves, N.Y.,1974,part. 6.
27 L.Westerberg et.al.: Phys. Rev. C18 (1978), 796.
28 T.J.M.Symons et. al.: Phys. Lett. 94B (1980), 131.
29 B.Jakobsson et. al.: Phys.Lett. 102B (1981), 121.
30 G.Claesson et. al.: Phys. Lett. 251B (1990), 23.